Important role of non-ideal effects in peeling-ballooning stability of spherical tokamaks

A. Kleiner[1], N.M. Ferraro[1], G.P. Canal[2], A. Diallo[1], A. Kirk[3], L. Kogan[3], S.F. Smith[3]

[1] *Princeton Plasma Physics Laboratory, Princeton, New Jersey 08543, United States*

[2] *Instituto de Física, Universidade de São Paulo, São Paulo CEP 05508-090, Brazil*

[3] *CCFE Culham Science Centre, Abingdon, Oxon, OX14-3DB, United Kingdom*

Edge-localized modes (ELMs) have been observed in a wide range of tokamaks operating in H-mode [1]. These periodic relaxations at the plasma edge do not only limit the performance of present day tokamaks, but can be dangerous for the plasma facing components in reactor-scale machines. The peeling-ballooning (PB) model [2] has been successfully employed to calculate the stability limits associated with ELMs in conventional aspect ratio machines, such as DIII-D [3]. PB modes are driven unstable by large current density and pressure gradients in the edge pedestal. Stability thresholds for PB modes are typically calculated within the frame of ideal-MHD, for example with the ELITE code. However, the predicted ideal-MHD stability limits often do not agree with experimental observations in plasma discharges in spherical tokamaks (STs), such as NSTX [4]. Some MAST discharges were found to be located on the ballooning stability boundary [5]. A distinctive advantage of spherical tokamaks is enhanced (ideal) MHD stability. STs can operate at higher normalized pressure and higher bootstrap current fractions, and are thus promising candidates for economical fusion reactors. A more accurate edge stability model is needed to understand pedestal physics in low-aspect ratio tokamaks, and to obtain a predictive pedestal structure model. We show that non-ideal physics, particularly resistivity, can significantly alter peeling-ballooning stability thresholds in spherical torus configurations, such as NSTX and MAST.

We first focus on ELMing standard H-mode NSTX discharge 132543, which exhibits type-I ELMs. We take a kinetic EFIT reconstruction as initial conditions for the simulations. The electron density n_e and electron temperature T_e measurements are averaged through the last 20% of the inter-ELM period to obtain a better spatial resolution. In order to calculate the stability limits, the edge current density and pressure are varied with the Varyped tool, creating a two-dimensional parameter space around the reconstructed equilibrium. The simulations with

the M3D-C1 code [6, 7] employ a single-fluid enhanced-MHD model [8]

$$\begin{aligned}
\frac{\partial \rho}{\partial t} + \nabla \cdot (\rho \mathbf{u}) &= 0, \\
\rho \left(\frac{\partial \mathbf{u}}{\partial t} + \mathbf{u} \cdot \nabla \mathbf{u} \right) &= \mathbf{J} \times \mathbf{B} - \nabla p - \nabla \cdot \Pi, \\
\frac{\partial p}{\partial t} + \mathbf{u} \cdot \nabla p + \Gamma p \nabla \cdot \mathbf{u} &= (\Gamma - 1) \left[\eta J^2 - \nabla \cdot \mathbf{q} - \Pi : \nabla \mathbf{u} \right], \\
\mathbf{E} &= -\mathbf{u} \times \mathbf{B} + \eta \mathbf{J}, \\
\mathbf{J} = \frac{1}{\mu_0} \nabla \times \mathbf{B} \quad , \quad \frac{\partial \mathbf{B}}{\partial t} &= -\nabla \times \mathbf{E},
\end{aligned} \tag{1}$$

where, as usual, $\mathbf{B}$ denotes the magnetic field, p the pressure, ρ the ion mass density, $\mathbf{u}$ the fluid velocity, $\mathbf{J}$ the current density, $\mathbf{E}$ the electric field, η the resistivity, Π the viscous stress tensor and $\mathbf{q}$ the heat flux density.

Similar to previous observations in ELMing NSTX discharges, Fig. 1 shows that the ideal-MHD models [ELITE and ideal limit (10% of Spitzer resistivity) in M3D-C1] predict PB modes to be stable in NSTX discharge 132543. However, when Spitzer resistivity is taken into account the unstable domain expands considerably and the discharge is located on the unstable side of the stability boundary as seen in Fig. 1c. To allow for a meaningful comparison with ELITE the M3D-C1 computations include diamagnetic effects in terms of the growth rate normalization. A mode is considered unstable if $\gamma_{\mathrm{MHD}} > \omega_{*\mathrm{eff}}/2$, and thus the stability boundary is given as $\frac{\gamma_{\mathrm{MHD}}}{\omega_{*\mathrm{eff}}/2} = 1$, with $\omega_{*\mathrm{eff}} = \frac{n}{e_i n_i} \frac{\mathrm{d}p_i}{\mathrm{d}\psi}$ being the maximum of the ion diamagnetic frequency in the pedestal (n is the toroidal mode number, subscript i denotes the main ion species and ψ is the poloidal flux). A considerable expansion of the unstable region towards lower values of edge current density and pressure is also found for ELMing NSTX discharges 139037 and 139047 when Spitzer resistivity is taken into account. In all of these cases the ideal-MHD calculations locate the experimental point on the stable side, while the resistive simulations indicate PB instability consistent with the occurrence of ELMs in the experiment. A more detailed discussion of the resistive scaling in NSTX is presented in Ref. [9].

While plasma rotation typically has a negligible effect on peeling-ballooning stability in the ideal-MHD model in conventional aspect ratio, this might not be the case in NSTX. In our simulations we initialize the fluid velocity with the measured toroidal ion rotation, but we do not modify the equilibrium to include centrifugal effects. For the considered NSTX cases, finite plasma rotation suppresses ideal core modes, but does not significantly affect edge stability. This was confirmed with further simulations based on the measured $\mathbf{E} \times \mathbf{B}$ velocity, where the growth rates changed only marginally.

Non-ideal effects other than resistivity are found to have a weaker impact on the stability

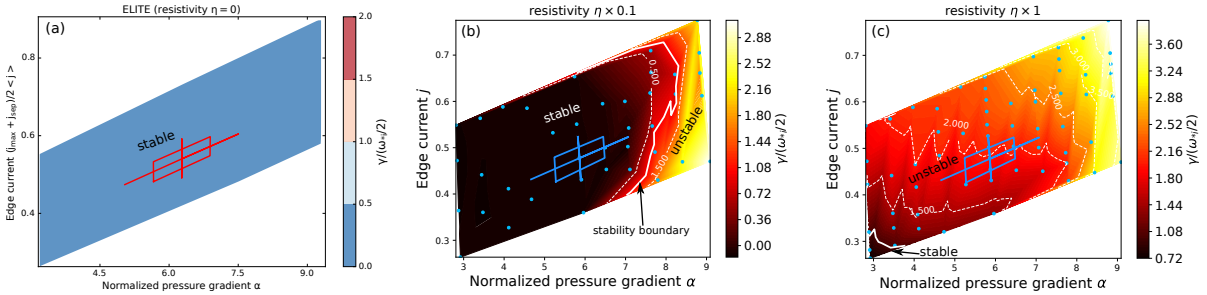

Figure 1: *Peeling-ballooning stability boundary and normalized growth rate $\gamma/(\omega_{*i}/2)$ of the most unstable mode calculated for equilibrium variations of NSTX discharge 132543 with (a) the ideal-MHD code ELITE. (b) M3D-C1 in the ideal limit. (c) M3D-C1 using Spitzer resistivity. The bold solid lines represent the stability boundary and the cross shows the experimental point. Reproduced from [9].*

boundary. As expected, finite-Larmor radius effects are stabilizing and in NSTX 132543 move the stability boundary closer to the operational point. This can explain why this point is experimentally accessible. The details will be subject to future publication.

To study the effect of resistivity η on peeling-ballooning stability limits in MAST, we consider ELMing single-null diverted discharge 29782. Fig. 2 shows the growth rate γ normalized by the Alfvén frequency ω_A for toroidal mode numbers $n = 1-20$ calculated with M3D-C1 in the ideal limit (10% of Spitzer resistivity) and with Spitzer resistivity. While some dependency of γ on η is observed, the scaling seems weaker compared to the observations in NSTX. Different to the ELMing NSTX cases the modes are already unstable in the ideal limit. These results were obtained with simple profiles for n_e and T_e and are thus preliminary. Current simulations are being carried out with the experimental profiles, and this will be followed by computing an equilibrium variation to determine the stability boundary. These results are subject to future publication.

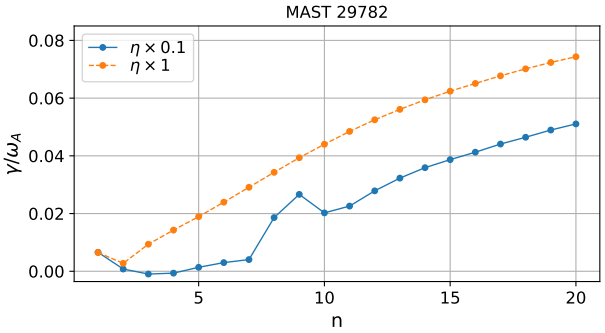

Figure 2: *Normalized growth rate γ/ω_A as a function of toroidal mode number n for MAST 29782 in the ideal limit ($\eta \times 0.1$) and with Spitzer resistivity ($\eta \times 1$).*

The stability limits calculated in the ideal-MHD limit with M3D-C1 have been benchmarked with a conventional aspect ratio discharge, and the effect of resistivity has also been investigated. For this study DIII-D discharge 147105 was considered during an ELMing phase at 3750 ms. The stability boundary calculated with ELITE and with M3D-C1 in the ideal limit agree rea-

sonably well. Resistivity causes the stability boundary to shift only moderately to lower values of edge pressure and current density, such that the ideal-MHD model can be considered to well describe PB stability limits in these cases [9]. For conventional aspect ratio machines it is typically found that modes on the pressure-limited side have ballooning character, while modes on the peeling-side have external-kink character. This is also true for the DIII-D discharge studied here. However, the resistive modes in NSTX show a ballooning character throughout the unstable domain, including the peeling side.

While resistivity appears to be important for peeling-ballooning stability in low-aspect ratio devices, it is not yet clear if this is a pure result of the aspect ratio itself or other physical parameters, such as collisionality, plasma current or pedestal width. This is currently under investigation. Future work will focus on ELM-free discharges in NSTX and MAST, as well as the impact of two-fluid effects on peeling-ballooning stability.

Acknowledgments

The authors thank Orso Meneghini, Tom Osborne, Sterling Smith and Phil Snyder for useful discussions. This research used resources of the National Energy Research Scientific Computing Center, which is supported by the Office of Science of the U.S. Department of Energy under Contract No. DE-AC02-05CH11231. This work was supported by the U.S. Department of Energy under contracts DE-AC02-09CH11466, DE-FC02-04ER54698 and the Department of Energy early career research program. The United States Government retains a non-exclusive, paid-up, irrevocable, world-wide license to publish or reproduce the published form of this manuscript, or allow others to do so, for United States Government purposes.

References

[1] A. W. Leonard, Phys. Plasmas **21**, 090501 (2014)

[2] H.R. Wilson et al, Plasma Phys. Control. Fusion **48**, A71 (2006)

[3] K. Burrell et al, Nucl. Fusion **49**, 085024 (2009)

[4] A. Diallo et al, Nucl. Fusion **53**, 093026 (2013)

[5] A. Kirk et al, Plasma Phys. Control. Fusion **51**, 065016 (2009)

[6] S.C. Jardin, J. Comp. Phys. 200:133, (2004)

[7] N.M. Ferraro et al, Phys. Plasmas **23**, 056114 (2016)

[8] J. Breslau et al, Phys. Plasmas **16**, 092503 (2009)

[9] A. Kleiner et al, Nucl. Fusion **61**, 064002 (2021)